Structural disorder and electronic hybridization in $Ni_cMg_{1-c}O$ solid solutions probed by XANES at the oxygen K edge

Dongliang Chen[1], **Jun Zhong**[1], **Wangsheng Chu**[1], **Ziyu Wu**[1,2,5],
Alexei Kuzmin[3], **Nina Mironova-Ulmane**[3] and **Augusto Marcelli**[4]

[1] Institute of High Energy Physics, Chinese Academy of Sciences, Beijing 100049,
People's Republic of China
[2] National Synchrotron Radiation Laboratory, University of Science and Technology of China,
Hefei 230026, People's Republic of China
[3] Institute of Solid State Physics, University of Latvia, Kengaraga 8, LV-1063 Riga, Latvia
[4] Laboratori Nazionali di Frascati, Istituto Nazionale di Fisica Nucleare, PO Box 13, 00044
Frascati, Italy

E-mail: wuzy@ihep.ac.cn

Abstract

A series of $Ni_cMg_{1-c}O$ solid solutions has been studied for the first time looking at the structural disorder by means of x-ray absorption near-edge-structure (XANES) spectroscopy at the oxygen K edge. The experimental XANES signals were analysed within the full multiple scattering formalism and were interpreted taking into account clusters of up to 15 coordination shells around an absorbing oxygen atom. The substitution of nickel atoms by magnesium atoms results in a dramatic decrease of the empty density of states in the conduction band close to the Fermi level due to an exchange of the 3d(Ni)–2p(O) interaction with 3p(Mg)–2p(O). Besides, a simultaneous small decrease of the 3d(Ni)–2p(O) hybridization is also induced by the lattice expansion, determined by the difference in ionic radii between nickel and magnesium ions.

1. Introduction

Transition metal oxides are materials which offer a huge number of applications; nevertheless, the knowledge of the atomic and electronic structure of simple transition metal oxides such as NiO is far from being exhaustive. Nickel oxide (NiO) is a wide-gap ($E_g \sim 4$ eV) charge-transfer insulator, whose anomalous electronic structure and magnetic properties, strongly influenced by correlation, have been known for a long time, but it still attracts a lot of interest and attention [1]. NiO has a rock-salt-type crystal structure in the paramagnetic

[5] Author to whom any correspondence should be addressed.

phase, whereas below the Nèel temperature $T_N = 523$ K [2], it undergoes a paramagnetic-to-antiferromagnetic transition, accompanied by a weak cubic-to-rhombohedral distortion [3]. In order to modify the electronic and magnetic properties of NiO in a controlled way, we considered the replacement of nickel with ions of similar size such as Mg, obtaining a continuous set of $Ni_cMg_{1-c}O$ diluted antiferromagnet solid solutions. These latter represent an interesting class of materials, whose crystallographic structure is closely related to their magnetic properties [4]. Actually the $Ni_cMg_{1-c}O$ solid solution is a prototype of a diluted face centered cubic (fcc) antiferromagnet, whose magnetic properties at room temperature change with composition (c) from an antiferromagnetic-like behaviour of pure NiO, to a paramagnetic-like behaviour at $c \approx 0.6$, and, finally, to the diamagnetic-like behaviour of MgO [5, 6]. The complete magnetic phase diagram of the $Ni_cMg_{1-c}O$ system can be found in [5, 6].

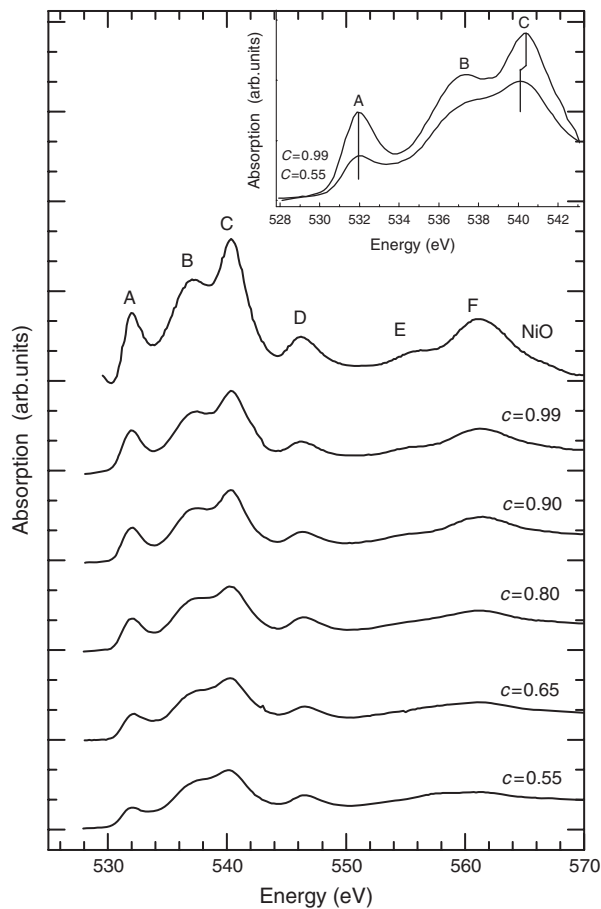The magnetic interactions in $Ni_cMg_{1-c}O$ solid solutions are characterized by two super-exchange interactions, the nearest-neighbour (NN) one, J_{NN}, and the next-nearest-neighbour (NNN) one, J_{NNN}, which couple nickel ions via an oxygen ion [7]. The exchange interactions J_{NN} and J_{NNN} are determined by the intermixing of the 3d(Ni) and 2p(O) states, which can be directly probed by x-ray absorption near-edge structure (XANES) spectroscopy. Indeed the XANES technique is sensitive to the variation of the partial and local electronic empty density of states. Moreover, XANES is sensitive to local atomic structure parameters such as site symmetry, interatomic distances, bond angles, coordination numbers, thermal vibrations and static disorder.

The hybridization phenomenon between 3d(Ni/Co) and 2p(O) states in two related $Ni_cMg_{1-c}O$ and $Co_cMg_{1-c}O$ solid solutions has been studied previously [7–9]. For transition metals (TMs) like Ni or Co, the K-edge x-ray absorption (the transition 1s $\rightarrow$ 3d) is dipole forbidden, and therefore only a weak pre-edge peak is detectable in the experimental spectra [7, 8]. Its origin is due to an interplay between two effects: (1) a hybridization of 3d(Ni) and 2p(O) states [7, 8], and (2) the quadrupolar allowed transition 1s $\rightarrow$ 3d($e_g \downarrow$) [9, 10]. At the K edge of the TM the small intensity of the pre-edge structure makes an accurate comparison of its intensity variation along the solid solution series rather difficult. However, these states, originating from the hybridization of 3d(Ni) and 2p(O) states and located at the bottom of the conduction band, may be also probed at the oxygen K edge, corresponding to the dipole-allowed 1s $\rightarrow$ np transitions [11].

In the present study, a comparison between O K-edge XANES and multiple-scattering calculations has been used to investigate changes occurring in the structural and electronic properties of the $Ni_cMg_{1-c}O$ solid solutions upon dilution. We mainly focused the analysis on the variation of the XANES peak at around 532 eV in a region extremely sensitive to the 3d(Ni)–2p(O) mixing.

2. Experimental details

The $Ni_cMg_{1-c}O$ solid solutions with the compositions $c = 0.99, 0.90, 0.80, 0.65,$ and 0.55 were prepared using the following procedure. Amounts of aqueous solutions of $Mg(NO_3)_2 \cdot 6H_2O$ and $Ni(NO_3)_2 \cdot 6H_2O$ salts corresponding to the appropriate solid solution composition were mixed and slowly evaporated. The remaining dry 'flakes' were heated up to 770–870 K to completely remove the NO_2. The polycrystalline solid solution thus obtained was powdered and annealed for 100 h at 1470 K in air and then quickly cooled down to room temperature. X-ray structural and phase analyses were carried out to monitor the solid solutions prepared [12]. It was found that all $Ni_cMg_{1-c}O$ samples were single phase with a rock-salt structure and a lattice parameter depending nearly linearly on the composition; it increases slightly upon dilution from 4.1773 Å in pure NiO to 4.2113 Å in pure MgO [12].

Figure 1. Oxygen K-edge XANES spectra of polycrystalline NiO and $Ni_cMg_{1-c}O$ solid solutions with the following compositions: $c = 0.99$, 0.90, 0.80, 0.65, and 0.55. The inset shows the edge region comparison of the two extreme compositions.

Oxygen K-edge XANES spectra were collected at the Beijing Synchrotron Radiation Facility (BSRF) using the light emitted by the storage ring working at a typical energy of 2.2 GeV with an electron current of about 100 mA. Samples were loaded in an ultrahigh-vacuum (UHV) chamber and maintained in a background pressure of $\sim 5 \times 10^{-8}$ Pa. Spectra were collected using the total electron yield (TEY) mode, a surface-sensitive detection method with a typical probing depth of a few nanometres. The O K-edge XANES spectra were obtained by measuring the photocurrent directly from the samples at steps of 0.05 eV with a resolution of about 0.3 eV. Additional details of the experimental set-up for the O K-edge experiments can be found in [13].

3. Results

Figure 1 displays the oxygen K-edge XANES spectra of pure NiO and a series of $Ni_cMg_{1-c}O$ solid solutions. All the spectra have been normalized using the Cromer–Liberman calculations by the IFEFFIT code [14, 15]. Our XANES data for pure NiO are characterized by six main

features, labelled from A to F, in good agreement with the data of Nakai *et al* [16] and Kuiper *et al* [17]. The other spectra are those of the $Ni_cMg_{1-c}O$ solid solutions with the composition $c = 0.99, 0.90, 0.80, 0.65,$ and 0.55.
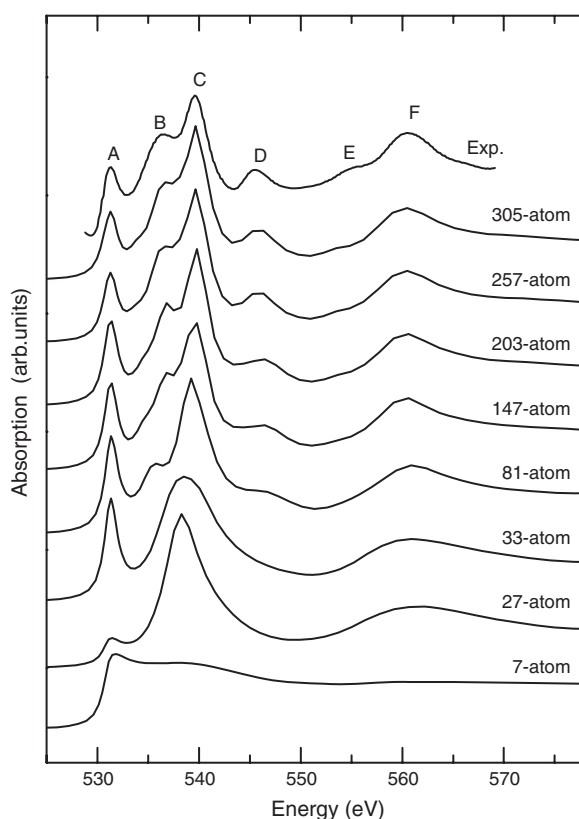
Looking at figure 1, we may divide the O K-edge XANES spectrum into three regions. The first region includes peak A, located at about 532 eV for all spectra: it is close in shape for all the spectra, including pure NiO, except for the intensity, which increases remarkably and monotonically with an increase of the nickel composition c. The second region, located at about 10 eV above the edge, is characterized by two multiple scattering (MS) peaks B and C. In this region MS features are typically affected by both medium- and long-range order, so the intensity and width of peaks B and C are correlated to the Mg content. The feature B is more sensitive to the dilution, decreasing with the increase of Mg, to become a small shoulder at the composition $c = 0.55$. Moreover, the energy position of feature C slightly shifts to low energy by about 0.4 eV with composition from $c = 0.99$ to 0.55. The third region extends up to 570 eV and contains three broad peaks labelled D, E, and F, respectively. The shape and energy position of the feature D are almost independent of dilution, while its amplitude decreases continuously, similarly to features E and F. These two latter almost disappear, merging into a unique large structure in the solid solutions with Ni concentration $c < 0.80$.

4. Calculation details

In order to understand the O K-edge XANES spectra of the $Ni_cMg_{1-c}O$ solid solutions, a detailed simulation of the oxygen K-edge XANES spectrum of the pure NiO has been performed using the *ab initio* real-space multiple-scattering (MS) code FEFF8.2 [18]. For the full-MS (FMS) analysis of the O K-edge XANES spectrum of NiO, we first determined the minimum size of the atomic cluster around the absorbing O atom, within which the photoelectron MS reproduces the near-edge structure of the XANES spectrum. Different NiO clusters have been considered in order to calculate the spectra to compare with the experimental data of pure NiO. The structural parameters of the bulk NiO refer to previous x-ray diffraction (XRD) results [12]. For the calculations performed with the FEFF8.2 code, we used the Hedin–Lundqvist model for the exchange potential with no energy shift, 0.6 eV of additional broadening and 15% muffin-tin overlap to reduce the discontinuity effects at the edges of the muffin tin and roughly determine the need for non-spherical corrections to the potential. The core–hole effect has been approximated by the final state rule, i.e. the potential of the final states is calculated self-consistently including a fully screened core–hole. The NiO cluster size up to nine shells (ie: 147 atoms) used in all FMS calculations is large enough to obtain accurate self-consistent field (SCF) calculations. Moreover, we found that the experimental data are better reproduced by including the core–hole effect in the calculations. From figure 2 it is clear that a cluster, having a radius of 8.5 Å and including at least 14 coordination shells (257 atoms), has to be taken into account to reproduce all features of the experimental spectrum of the pure NiO, indicating that a large cluster is necessary to describe the bulk properties of these TM oxides.

Derived from the highly correlated NiO, the $Ni_cMg_{1-c}O$ system forms a continuous series of solid solutions that conserves the rock-salt crystal structure, in which metal ions occupy the sites of the fcc lattice for any composition. The lattice parameters of $Ni_cMg_{1-c}O$, reported in the previous XRD work [12], were used in our XANES calculations, as shown in table 1.

In order to understand the variation of the O K-edge XANES signal on the composition in the $Ni_cMg_{1-c}O$ system as well as to characterize the geometry effect due to the lattice expansion occurring upon substitution of nickel with magnesium, we attempted to model the O K-edge XANES spectra by substituting the proper amount of nickel atoms with magnesium
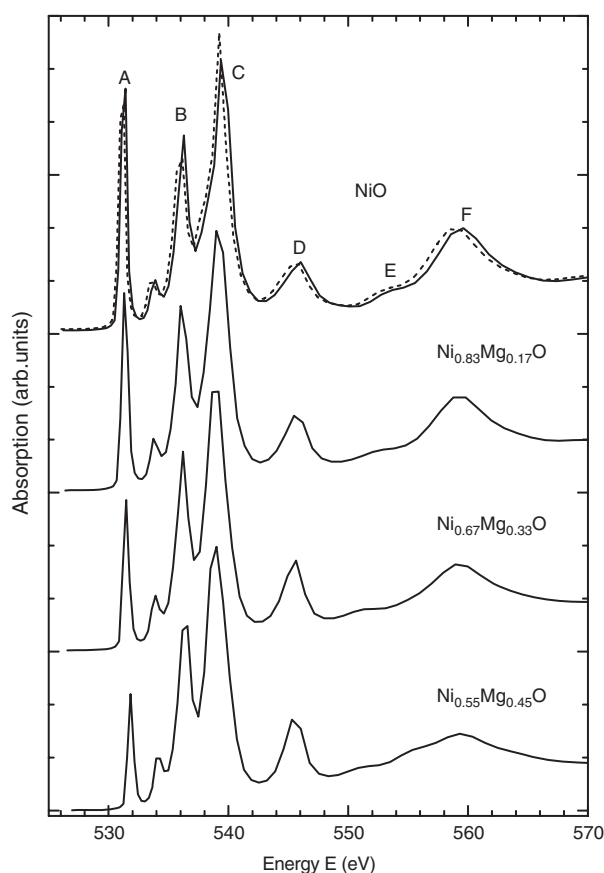
Figure 2. Comparison of the experimental O K-edge NiO XANES spectrum and theoretical simulations performed for increasing atomic clusters. The 305-atom cluster includes the central oxygen plus 6 Ni, 12 O, 8 Ni, 6 O, 24 Ni, 24 O, 12 O, 30 Ni, 24 O, 24 Ni, 8 O, 24 Ni, 48 O, 6 O and 48 Ni atoms for a total of 141 oxygen and 164 nickel atoms. All simulations have been broadened by 0.6 eV to take into account for both core–hole lifetime and experimental resolution.

Table 1. Lattice parameters of $Ni_cMg_{1-c}O$ compounds for different composition c [12].

Composition, c	1.00	0.83	0.67	0.55	0.50	0.00
Lattice parameter, a (Å)	4.1773	4.1822	4.1872	4.1906	4.1920	4.2113

ones (figure 3) and selecting the values of the lattice parameters from the previous XRD work [12], as summarized in table 1. As a result, three main effects are observed versus dilution going from NiO to $Ni_{0.55}Mg_{0.45}O$: (i) the intensity of peak A decreases by a factor two, (ii) peaks B and C appear closer by about 0.7 eV, and (iii) peak F becomes broad and for Ni concentration <0.67 it exhibits a shoulder on its low-energy tail that essentially smears the presence of peak E. These results are fully consistent with the experimental behaviour shown in figure 1. Due to the very small difference in the lattice parameters of pure NiO ($a = 4.1773$ Å) and MgO ($a = 4.2113$ Å) [12], the effect of the lattice parameter variation is small; however, as expected, it leads to a slight shift of the peak positions.
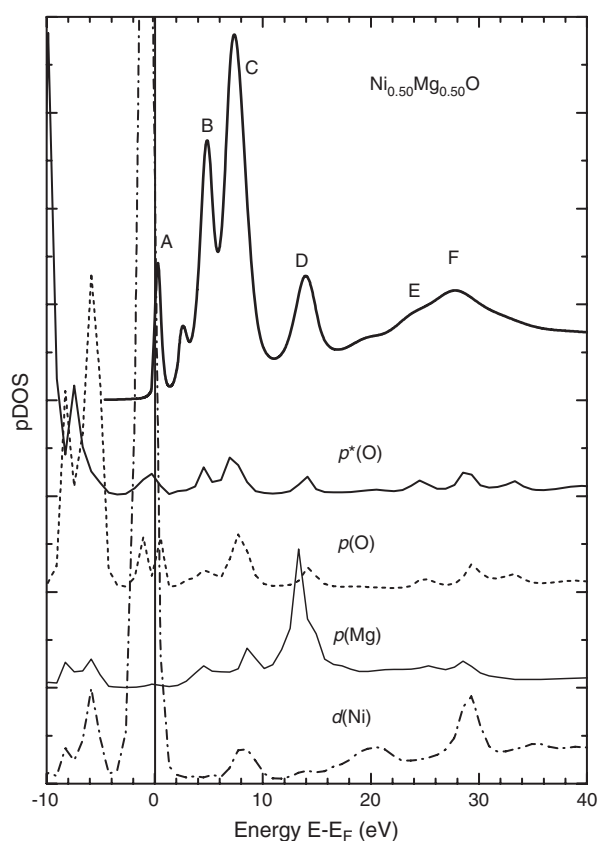
The importance of the core–hole effect and different atom type contributions on the XANES signal is evaluated in figure 4. Because XANES is sensitive to the local and empty

Figure 3. Composition dependence of the calculated O K-edge XANES in $Ni_cMg_{1-c}O$ solid solutions for a cluster of 8.5 Å radius (see text). Experimental peaks are labelled from A to F as in figure 1. The NiO XANES spectrum calculated with the value of the lattice parameter of pure MgO [12] is also shown (dashed line). To emphasize the contributions the simulations are not broadened.

density of states, the relevant partial densities of states (pDOSs) $p^*(O)$, $p(O)$, $p(Mg)$ and $d(Ni)$, calculated using the large $Ni_{0.50}Mg_{0.50}O$ cluster of 8.0 Å radius, are compared in figure 4 with the total XANES signal. The final-state oxygen p DOS is denoted by $p^*(O)$ and corresponds to the excited fully relaxed state with the core–hole at the 1s(O) level. Three main effects can be observed: (i) the influence of the core–hole effect on the p(O) DOS is rather small but is detectable, especially, at the top of the valence band (region from -10 to -5 eV), (ii) the hybridization between 2p(O) and 3d(Ni) states is relevant in the conduction band (region from -3 to $+3$ eV) and (iii) the 3p(Mg) states do not contribute at the bottom of the conduction band but give rise to a sharp peak at 13 eV above the Fermi level.

　　Finally, trying to understand the intensity behaviour of feature A versus composition in the $Ni_cMg_{1-c}O$ system as well as the geometry effect due to the lattice expansion occurring with the dilution, we calculated the O K-edge XANES spectra using a very simplified model, in which the six Ni atoms in the nearest-neighbour shell around the central oxygen atom were replaced by Mg atoms. The O K-edge XANES spectra were calculated using the lattice parameters of 4.1773 and 4.2113 Å for pure NiO and pure MgO, respectively [12]. As displayed
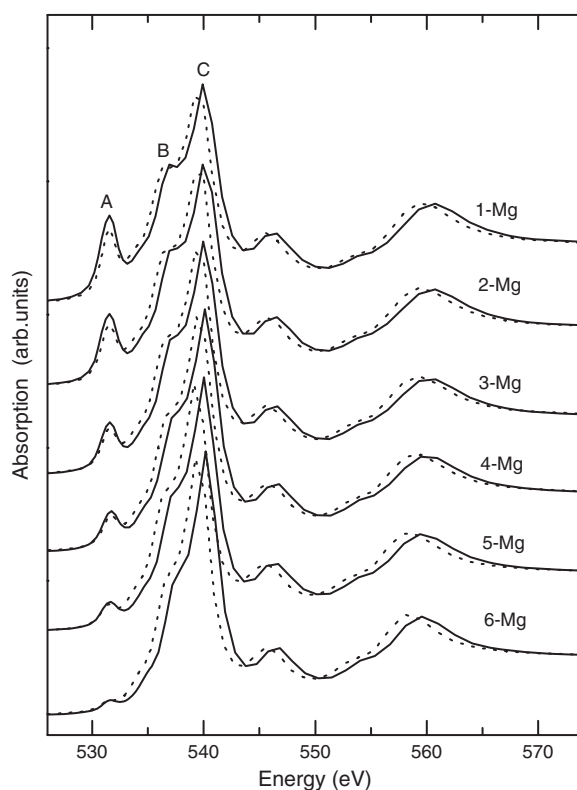
Figure 4. Comparison between p*(O), p(O), p(Mg) and d(Ni) partial density of states (pDOS) and the calculated O K-edge XANES in $Ni_{0.50}Mg_{0.50}O$. All spectra were calculated for a cluster of 8 Å radius and the position of the Fermi level is shown by a vertical solid line. Here p*(O) is the empty DOS corresponding to the excited relaxed state with the core–hole at the 1s(O) level.

in figure 5, an increase of the number of Mg atoms, while reducing the Ni ones, results in a strong decrease of the peak A intensity, whereas the overall shape of the XANES signals remains unchanged. The behaviour may be correlated to the difference between 3d(Ni)–2p(O) and 3p(Mg)–2p(O) hybridizations, being consistent with the difference in pDOS of Ni and Mg atoms shown in figure 4.

5. Discussion

First we will discuss the results for pure NiO. As shown in figure 2, FMS calculations at the O K edge in NiO have been carried out using different atomic clusters with an increasing number of atoms, from 7 (1 O and 6 Ni) to 305 (141 O and 164 Ni), until convergence was achieved. We have to underline also that the calculation associated with the largest clusters (14 shells including 257 atoms, and 15 shells including 305 atoms) do not significantly improve the results. A good agreement between theory and experiment already occurs for a NiO cluster size containing 14 shells (8.5 Å radius) around the photo-excited oxygen atom, showing that a relatively large cluster is required to simulate all details of an XANES spectrum for a cubic crystal with a large number of collinear atomic chains, as previously shown in other calculations of the same system or in other cubic structures [19, 20].

Figure 5. Composition dependence of feature A at the O K-edge XANES for the $Ni_cMg_{1-c}O$ solid solutions. Spectra have been calculated for clusters including 14 coordination shells around the central oxygen atom and correspond to a different number (from one to six) of Mg atoms replacing Ni in the first shell around the O ion. The lattice parameters used for these calculations are those of pure NiO (solid line) and of pure MgO (dotted line).

For the smallest cluster, composed of a central oxygen atom surrounded by six nickel atoms (forming a perfect octahedron), the calculated spectrum shown in figure 2 already contains a small peak A. This feature is associated with transitions from the O 1s electron to the empty antibonding O 2p states strongly hybridized with the empty 3d metal states, mainly localized at the Ni site. Its intensity and shape depend on the Ni site symmetry, the occupation number of the d levels, as well as the Ni–O bond length [19, 21–23]. On increasing the cluster size up to 27 atoms, e.g., adding two shells composed of 12 oxygen and 8 nickel atoms, two new features C and F appear, while no change occurs in the edge region. Only after the addition of an oxygen shell (6 O atoms) does the peak A become pronounced, in good agreement with the experimental data. Actually, the 33-atom cluster includes enough outer shells of oxygen atoms around the first neighbour Ni atoms to form six NiO_6 octahedra surrounding the central oxygen atom, so the molecular orbitals are the same as those occurring in a solid-state system, demonstrating also that solid-state effects play a relevant role in NiO [24]. However, the convergence of FMS calculations for peak A is achieved only with a cluster of 257 atoms of about 8.4 Å radius. We have also to underline here that peak A mainly probes the unoccupied density of states arising from the hybridization of the central O 2p orbitals with the nearest-neighbouring Ni 3d orbitals and this first O K resonance is also affected by the medium-range order of the system, similarly to what is also observed in α-Fe_2O_3 [21].

Features B and C, located at about 10 eV above the edge (figure 1), also reflect the p-type projected empty density of states. In this region, the oxygen 2p orbitals are hybridized with the Ni 4s and 4p bands and represent a region of accessible continuum state including the main peak (feature C) with the shoulder (feature B) on its low-energy side [21]. This broader structure can be associated with the O_h symmetry set up by the nearest oxygen neighbours that octahedrally surround the Ni atom [23]. The energy dispersion of the oxygen 2p character is due to the large covalence of NiO and may be the quantitative signature of the non-local charge transfer in the NiO solid solutions [24]. On increasing the cluster size, up to 6 shells (81 atoms), features B and D also appear but a reasonable agreement with experimental spectra is obtained for feature B only for a cluster including 10 shells, i.e., 171 atoms within 7.0 Å of the central oxygen atom. A larger cluster is necessary for feature D, confirming that both features B and D arise from medium- and/or long-range distributions. In contrast, a calculation based only on a 19-atom cluster (2 shells) already reproduces both features C and F well. FMS calculations support the interpretation that feature C is 'a scattering resonance' due to MS events up to infinite order, where the final state of the photoelectron is in the cage of the first oxygen shell while feature F can be mainly associated with single-scattering (SS) events occurring in the first oxygen shell [19]. Intrashell multiple scattering contributions within the first oxygen shell may also account for features C and F, while outer shells, i.e., atoms located at longer distance, contribute to features B and D, as occurs in other transition metal oxides such as α-Fe_2O_3 and MnO [21–23]. As already discussed in [16], a fairly large atomic cluster, e.g., more than 200 atoms, is necessary to reproduce feature E, a contribution due to long-range contributions assigned to SS processes between the absorber and atoms located in higher neighbouring shells.

Finally, one should point out that the appearance of main features in the O K-edge XANES upon an increase of the cluster size is primarily associated with the addition of the oxygen shells because of the higher scattering amplitude of oxygen atoms at lower energies with respect to nickel atoms.

Further, the variation of XANES upon substitution of nickel atoms with magnesium will be discussed. Based on the above results, the intensity of peak A in the spectra of the $Ni_cMg_{1-c}O$ systems (see figure 1) is correlated to the oxygen 2p weight in the conduction-band states with mainly Ni 3d character. Upon substitution of nickel atoms with magnesium, the number of 3d(Ni)–2p(O) interactions and the intensity of peak A decreases, since 3p(Mg)–2p(O) interactions contribute at about 10–15 eV above the Fermi level (see figure 4). A similar behaviour has also been observed in the $Li_xNi_{1-x}O$ system [17]. The intensity decrease of feature A upon dilution is clearly reproduced in figure 3 by FMS calculations, when the proper amount of nickel and magnesium atoms is taken in each coordination shell around the photoabsorber oxygen atom. Another possible source of the peak A intensity variation is due to a decrease of the 3d(Ni)–2p(O) hybridization due to an increase of the lattice parameter. The effect has been already observed and discussed in a previous XAS (x-ray absorbtion spectroscopy) study by Colliex *et al* [25] in iron oxides. Indeed, the O–Ni bond length in the $Ni_cMg_{1-c}O$ system depends almost linearly on the composition, showing a slight increase upon dilution by magnesium [7, 12]. However, the expected change of feature A induced by a lengthening of the O–Ni bond is very small if compared to that induced by the decrease of the number of O–Ni bonds (figures 3 and 5).

Kurata *et al* [21] and de Groot *et al* [24] have also observed a monotonic decrease of the intensity of peak A in the transition metal series as a function of the number of the accessible vacant d states. However, we do not observe a similar behaviour because all ions in the $Ni_cMg_{1-c}O$ system preserve their valence state versus composition.

On decreasing the nickel content from $c = 1.0$ to 0.55, the full width at half maximum (FWHM) of feature A narrows slightly by about 10%, in good agreement with the density

of states calculations of the $Ni_cMg_{1-c}O$ system obtained with *ab initio* periodic unrestricted Hartree–Fock calculations by Towler *et al* [26]. These calculations show that the widths of the Ni 3d bands, i.e., the e_g and t_{2g} components, are determined by the intensity of super-exchange interactions via the oxygen with a small contributions by direct Ni–Ni overlap. Indeed, the width of the Ni 3d band decreases slightly with an increase of the number of magnesium neighbours, leading to a narrowing of feature A [7, 26] because of the charge transfer between oxygen and nickel.

As shown in figure 3, peak B shifts slightly closer to peak C, making it less resolved. The energy position of peak C slightly shifts toward low energies due to the lattice expansion. Both trends are in agreement with the experimental behaviour shown in figure 1. The features B and C are associated to oxygen 2p orbitals hybridized with both Ni 4s4p and Mg 3p orbitals. Looking at figure 5, we recognize that upon increasing the Mg content, while peak A decreases, peak C slightly increases. Changes in the shoulder B are almost negligible, but the behaviour is consistent with the data of figure 4, showing that the maximum of the O 2p empty density of states occurs in correspondence with peak C. The assignment is also supported by the data of the O K edge in MgO (see figure 3 in [27]), showing that the maximum of the empty DOS is at the same energy as peak C.

Looking at peak D, its shape and energy position are almost independent of dilution. This feature was assigned in [21] to intershell multiple scattering after addition of a third oxygen coordination shell. Our FMS calculations for $Ni_cMg_{1-c}O$ indicate that peak D is weakly sensitive to the presence of the Mg atoms although the 3p(Mg) states peak strongly in this region (figure 4). The effect is weak and does not contribute significantly to XANES features (figure 1).

The last two features, E and F, both experience a broadening for low nickel contents (figure 1). Moreover, feature E slowly shifts toward lower energies and nearly disappears upon dilution with magnesium. Indeed, it originates from long distant shells, e.g., MS contributions (figure 2), sensitive to the chemical and structural disorder in the $Ni_cMg_{1-c}O$ system [7, 12]. Peak F originates from the scattering inside the first oxygen coordination shell [21]. Its position follows the expected increase of the lattice parameter in the $Ni_cMg_{1-c}O$ system upon dilution as probed by both XRD and EXAFS [7, 12] (figure 3). The broadening of peak F at low Ni compositions can be associated with local environment distortions previously observed [7, 12].

Summarizing, although to a different degree, almost all XANES features are sensitive to the disorder and reveal at different levels both electronic and structural information.

6. Conclusion

Oxygen K-edge x-ray absorption spectroscopy measurements were performed for the first time in polycrystalline $Ni_cMg_{1-c}O$ solid solutions with $c = 0.99$–0.55 and they are discussed within the FMS formalism, based on the FEFF8.2 code. The one-electron full multiple-scattering XANES theory is fully adequate in these solid solutions. FMS calculations are able to reproduce all the main features of XANES spectra for a sufficiently large cluster size, and the shells containing oxygen atoms give the main contributions to the O K-edge XANES.

FMS calculations show that the intensity of the first peak A, located at the bottom of the conduction band, decreases dramatically when magnesium atoms replace nickel, thus decreasing the number of 3d(Ni)–2p(O) interactions. The effect of the lattice expansion on the peak A intensity is negligible; however, due to the narrowing of the Ni 3d band, a small decrease of the width of peak A versus dilution is determined by the increase of Mg neighbours.

Broadening of the other XANES features versus dilution by Mg ions occurs due to the difference between Ni and Mg scattering amplitudes. The effect of lattice parameter variation is small but not negligible when compared to the variations induced by ion substitutions. Among

the XANES features, the D one is more sensitive to the medium-range order and the decrease of its intensity versus dilution is partially compensated by the contribution of Mg p states located at about 10–15 eV above the Fermi level.

The analysis performed on this solid solutions shows that XANES spectroscopy is an almost unique technique capable of obtaining information on the geometrical atomic arrangements in a cluster of a few angstroms radius together with electronic properties associated with the local and partial nature of its final-state configuration(s). This last aspect is particularly relevant in correlated materials like NiO and other transition metal oxides [11].

Acknowledgments

References

[1] Hufner S 1994 *Adv. Phys.* **43** 183
[2] Seehra M S and Giebultowicz T M 1988 *Phys. Rev.* B **38** 11898
[3] Massarotti V, Capsoni D, Berbenni V, Riccardi R and Marini A 1991 *Z. Naturf.* a **46** 503
[4] Furdyna J K and Kossut J (ed) 1988 *Diluted Magnetic Semiconductors* (New York: Academic)
[5] Menshikov A Z, Dorofeev Y A, Klimenko A G and Mironova N A 1991 *Phys. Status Solidi* b **164** 275
[6] Feng Z and Seehra M S 1992 *Phys. Rev.* B **45** 2184
[7] Kuzmin A, Mironova N, Purans J and Rodionov A 1995 *J. Phys.: Condens. Matter* **7** 9357
[8] Kuzmin A, Mironova N and Purans J 1997 *J. Phys.: Condens. Matter* **9** 5277
[9] Kuzmin A, Purans J and Kalendarev R 2005 *Phys. Status Solidi* c **2** 665
[10] Hill J P, Kao C C and McMorrow D F 1997 *Phys. Rev.* B **55** R8662
[11] Groot F de 2001 *Chem. Rev.* **101** 1779
[12] Kuzmin A and Mironova N 1998 *J. Phys.: Condens. Matter* **10** 7937
[13] Liu F Q, Ibrahim K, Qian H J, Yang Y, Tao X P, Jia J F and Dong Y H 1996 *J. Electron. Spectrosc. Relat. Phenom.* **80** 409
[14] Newville M 2001 *J. Synchrotron Radiat.* **8** 322
[15] Cromer D T and Liberman D 1970 *J. Chem. Phys.* **53** 1891
[16] Nakai S, Mitsuishi T, Sugawara H, Maezawa H, Matsukawa T, Mitani S, Yamasaki K and Fujikawa T 1987 *Phys. Rev.* B **36** 9241
[17] Kuiper P, Kruizinga G, Ghijsen J, Sawatzky G A and Verweij H 1989 *Phys. Rev. Lett.* **62** 221
[18] Ankudinov A L, Ravel B, Rehr J J and Conradson S D 1998 *Phys. Rev.* B **58** 756
[19] Wu Z Y, Liu C M, Guo L, Hu R, Abbas M I, Hu T D and Xu H B 2005 *J. Phys. Chem.* B **109** 2512
[20] Gunnella R, Benfatto M, Natoli C R and Marcelli A 1990 *Solid State Commun.* **76** 109
[21] Wu Z Y, Gota S, Jollet F, Pollak M, Gautier-Soyer M and Natoli C R 1997 *Phys. Rev.* B **55** 2570
[22] Kurata H, Lefevre E, Colliex C and Brydson R 1993 *Phys. Rev.* B **47** 13763
[23] Groot F M F de, Grioni M, Fuggle J C, Ghijsen J, Sawatzky G A and Petersen H 1989 *Phys. Rev.* B **40** 5715
[24] Duda L C, Schmitt T, Magnuson M, Forsberg J, Olsson A, Nordgren J, Okada K and Kotani A 2006 *Phys. Rev. Lett.* **96** 67402
[25] Colliex C, Manoubi T and Ortiz C 1991 *Phys. Rev.* B **44** 11402
[26] Towler M D, Allan N L, Harrison N M, Saunders V R and Mackrodt W C 1995 *J. Phys.: Condens. Matter* **7** 6231
[27] Davoli I, Tomellini M, Marcelli A, Bianconi A and Fanfoni M 1986 *Phys. Rev.* B **33** 2979